JOURNAL OF Materials CHEMISTRY

A rapid chemical route to niobates: hydrothermal synthesis and transport properties of ultrafine $Ba_5Nb_4O_{15}$

Hui Zhao, Shouhua Feng,* Wei Xu, Yanhui Shi, Yachun Mao and Xiangrong Zhu

Key Laboratory of Inorganic Synthesis and Preparative Chemistry, Jilin University, Changchun 130023, P. R. China

Received 3rd December 1999, Accepted 14th January 2000

A rapid synthetic route to ultrafine $Ba_5Nb_4O_{15}$ powders is reported in which the compound is hydrothermally prepared at 240 °C in 3 h. It was characterized by powder X-ray diffraction, transmission electron microscopy, Raman, IR spectroscopy and thermal analysis–thermogravimetry. The influences of various hydrothermal conditions such as reaction time and temperature on the formation, morphology and grain size of products were investigated. The product has a narrow distribution of particle size with particles *ca.* 100 nm in diameter. The electrical conductivity of $Ba_5Nb_4O_{15}$ was investigated from 300 to 800 °C by a complex impedance technique under different atmospheres. A mixed proton and electron conductivity was observed in a wet atmosphere. Electronic conduction originates from oxygen loss and ionization of oxygen vacancies, whereas proton conduction arises from reaction of water molecules with oxygen vacancies. The conductivity and corresponding activation energy for $Ba_5Nb_4O_{15}$ at 800 °C were 1.1×10^{-4} S cm^{-1} and 0.62 eV, respectively.

1 Introduction

High temperature proton conductors are useful materials in many fields such as solid oxide fuel cells (SOFCs), chemical sensors, electrolytes for hydrogen production and high temperature membrane reactors. Among these materials $BaCeO_3$ has been widely investigated. However its application is limited due to its structural instability in wet atmospheres.[1] Recently perovskite-like niobates, $Sr_2Sc_{1+x}Nb_{1-x}O_{6-\delta}$ and $Ba_3Ca_{1+x}Nb_{2-x}O_{9-\delta}$, have been found to show good high temperature proton conduction properties.[2] All these factors prompted us to study other related niobates. $Ba_5Nb_4O_{15}$ is a layered perovskite-related oxide.[3] The dielectric and luminescence properties of this compound have been investigated and it is found to be a useful material in microwave communication.[4–8] Recently, Pagola and coworkers investigated the IR and transport properties of stoichiometric and oxygen deficient $Ba_5Nb_4O_{15}$, and reported semiconducting properties for the oxygen deficient phase at low temperature.[9]

Traditionally, $Ba_5Nb_4O_{15}$ is produced from high temperature solid state reactions at 1200 °C with the resulting aggregate requiring a subsequent milling process. Since fabrication of advanced and complex electronic components always requires homogeneous and pure powders with fine and uniform particle sizes[10] an alternative synthesis procedure is needed. The hydrothermal technique, which has been applied to the synthesis of complex oxides and fluorides is characterised by mild synthesis temperature, chemical homogeneity, high purity and controlled size and morphology which tends to improve or dramatically change the physical properties of the final products.[11–15]

We report here, the hydrothermal synthesis and high temperature transport properties of $Ba_5Nb_4O_{15}$ ceramic powders.

2 Experimental

The starting materials for the synthesis of $Ba_5Nb_4O_{15}$ were Nb_2O_5(A.R) and $Ba(OH)_2{\cdot}8H_2O$(A.R). In a typical synthesis procedure, 1.26 g $Ba(OH)_2{\cdot}8H_2O$ were dissolved in 10 ml distilled deionized water to form a solution, to which 0.26 g Nb_2O_5 powder was added with stirring. The formed mixture was placed in a sealed Teflon lined stainless steel autoclave and heated at 240 °C for 3 h. The crystalline powder product was filtered off, washed with deionized water and dried in air at ambient temperature.

The product was characterized by X-ray diffraction (XRD) on a Rigaku D/Max-rA diffractometer with a rotating target using Ni-filtered Cu-Kα radiation at room temperature. The XRD data for indexing and cell-parameter calculation were collected over range 10–60 °C in a scan mode with a step length of 0.02° and a preset time of 4 s per step. Silicon was used as an internal standard.

The morphology of the crystalline product was observed by TEM with a Hitachi H-8100IV transmission electron microscope. Thermogravimetry and differential thermal analysis were conducted on Perkin-Elmer DTA-7000, TGA-7PC series thermal analysis instrument in air with a heating rate of 10 °C min^{-1}. IR spectra were obtained with a Nicolet 5DX spectrometer using the KBr pellet technique. In order to avoid the presence of absorbed water in the KBr, the pellet was dried using an IR lamp under a dry air stream. Raman spectra were collected at room temperature in the back-scattering geometry on a Spex double monochrometer coupled with a conventional photon counting system.

Ionic conductivity measurements were performed by a complex impedance method at frequencies ranging from 1 Hz to 1 MHz on a Solartron 1260 impedance/gain-phase analyzer. The electrical conductivity was measured on sintered disks under dry or wet oxygen, air or nitrogen atmospheres. The oxide powders were pressed into a compact pellet (10 mm in diameter and 2 mm in thickness) under 35 MPa and the disc was sintered at 1000 °C for 4 h in air. Platinum paste was painted on two sides of the disc to provide the electrodes, and then the disc was sintered at 800 °C for 30 min to remove the solvent. Since the oxide lost some oxygen above 600 °C, all samples, before measurements, were annealed in air at 400 °C for 96 h.

DOI: 10.1039/a909554c

3 Results and discussion

3.1 Hydrothermal synthesis

In the hydrothermal synthesis of $Ba_5Nb_4O_{15}$, the Ba/Nb mole ratio is a critical factor. When the Ba/Nb mole ratio is >2, pure phase $Ba_5Nb_4O_{15}$ as the only stable phase was obtained. When the ratio of Ba/Nb is <2, however, unreacted Nb_2O_5 and some amorphous phases were found. Clearly, in the reaction process, excess $Ba(OH)_2$, which serves as both reactant and mineralizer, is critical.

Various crystallization temperatures (180–240 °C) were examined at a fixed Ba/Nb ratio of 2 and a reaction time of 3 h. Fig. 1(a) shows the XRD patterns of some samples prepared at different temperatures. $Ba_5Nb_4O_{15}$ exists as a minor phase at 180 °C, and prolonging the reaction time (from 3 h to *ca.* 2 days) did not result in pure phase product. Pure $Ba_5Nb_4O_{15}$ is, however, obtained at 240 °C. Fig. 1(b) shows the XRD patterns of some samples formed at 240 °C for different times. The $Ba_5Nb_4O_{15}$ phase formed at 240 °C after 1 h and completion of crystallization required another 2 h. The influence of crystallization temperature and time on the formation of products follows the dissolution–recrystallization mechanism.[16] In the course of crystallization, initial amorphous $Nb(OH)_5{\cdot}xH_2O$ was formed. The crystallization reaction of amorphous $Nb(OH)_5{\cdot}xH_2O$ and $Ba(OH)_2$ was very dependent upon the crystallization temperature.

3.2 Structural characterization

The XRD data of hydrothermally synthesized $Ba_5Nb_4O_{15}$ can be indexed in the hexagonal system. The lattice constants calculated by least squares methods are $a=5.798$ Å and $c=11.771$ Å, slightly lower values than from ref. 17. This result could be ascribed to the existence of hydroxy groups in the hydrothermally synthesized products. A similar result has been observed in hydrothermally produced $BaTiO_3$ powders.

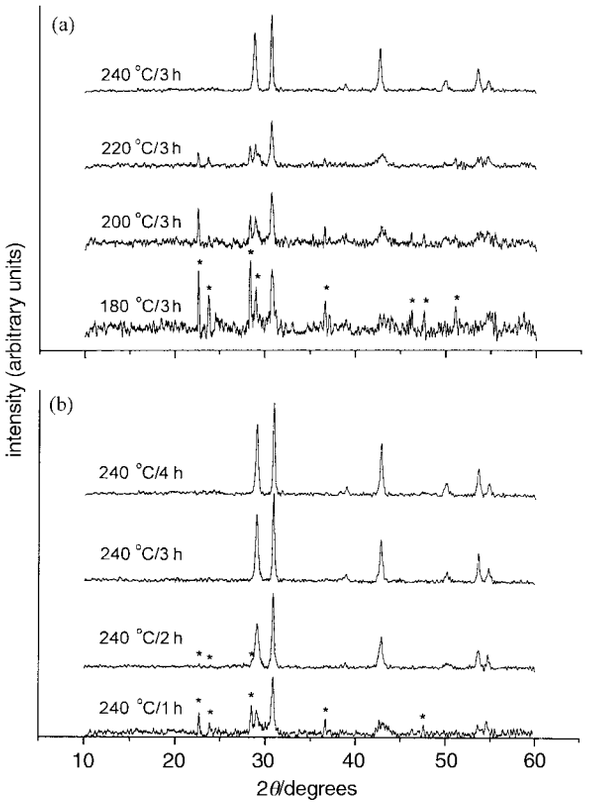

Fig. 1 XRD patterns of samples prepared at different temperatures for 3 h: 180, 200, 220 and 240 °C. (b) at 240 °C for different times: 0.5, 1, 2 and 3 h. An asterisk represents unreacted Nb_2O_5.

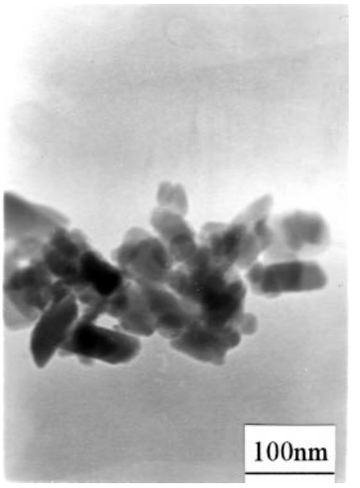

Fig. 2 TEM of $Ba_5Nb_4O_{15}$ hydrothermally synthesized at 240 °C for 3 h.

TEM photographs (Fig. 2) show the well crystallized morphology and a narrow particle size of *ca.* 100 nm.

Raman and IR spectra are shown in Fig. 3 and 4, respectively. The Raman spectrum shows two bands in the nondegenerate symmetric region (700–1000 cm^{-1}) at 795 cm^{-1} (strong) and 891 cm^{-1} (weak), corresponding to Nb–O stretching vibrations.[18] The IR spectrum shows one band in the same range. An IR band is observed at *ca.* 3700 cm^{-1} arising from ν(O–H)[19] which is eliminated on heating the sample at 1000 °C for 8 hours. This result further suggests that there are lattice water or surface hydroxy groups in the products prepared from particular hydrothermal systems.

The TG curve of $Ba_5Nb_4O_{15}$ in air (Fig. 5) shows physically absorbed water losses at *ca.* 150 °C. Another weight loss of $<1\%$ at *ca.* 600 °C indicates the loss of oxygen as observed for many other niobates.[20] No further weight loss is observed up to 800 °C. The second weight loss can be repeatedly observed if the sample is annealed in air after the measurements.

3.3 Transport properties

Fig. 6 shows the impedance plot of $Ba_5Nb_4O_{15}$ measured in air at 550 °C. A high frequency depressed semicircle is observed. The resistance of the sample corresponds to the intercept of the high frequency semicircle with the real axis. The temperature dependence of the conductivity under different atmospheres is shown in Fig. 7. It is observed that the plot presents two distinct linear regions, intersecting at 600 °C. Both lines obey the Arrhenius conductivity equation $\sigma=\sigma_0\exp(-\Delta E/kT)$.

The conductivity below 600 °C changes systematically as a

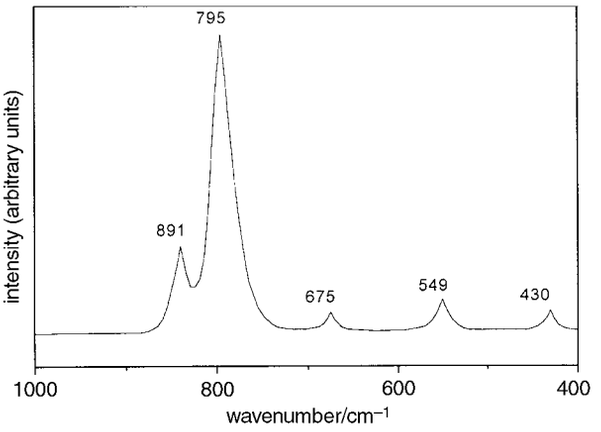

Fig. 3 Raman spectrum of $Ba_5Nb_4O_{15}$.

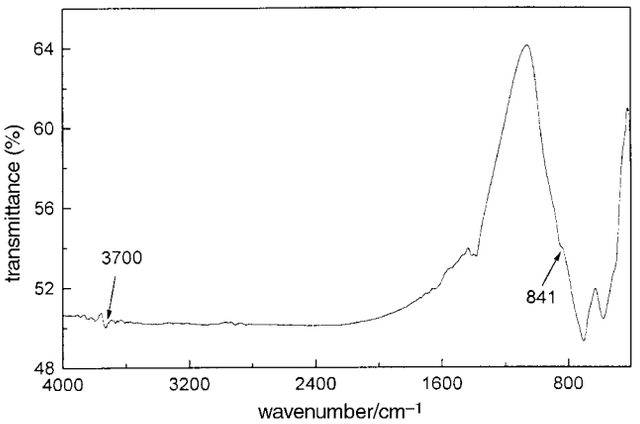

Fig. 4 IR spectrum of $Ba_5Nb_4O_{15}$.

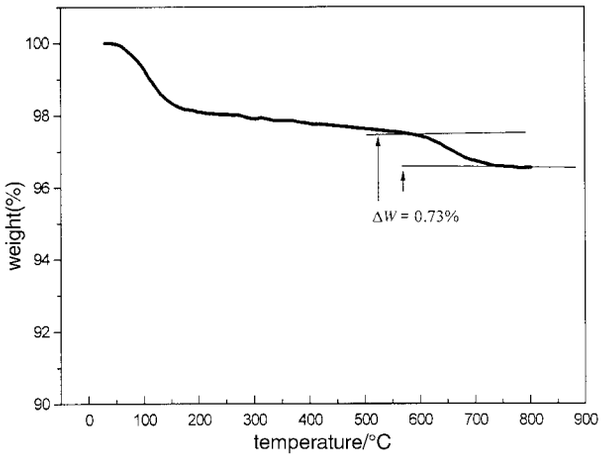

Fig. 5 TG curve of $Ba_5Nb_4O_{15}$ measured in air.

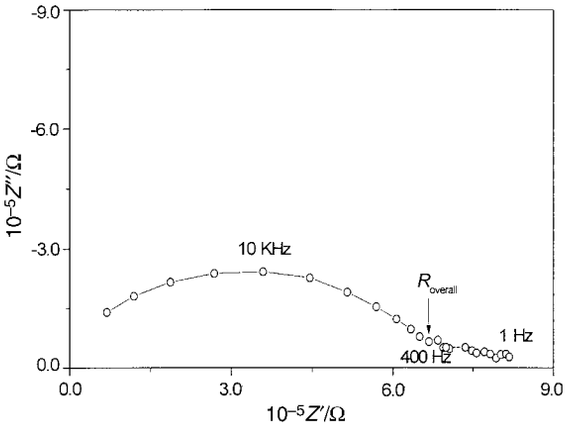

Fig. 6 Complex impedance plot for $Ba_5Nb_4O_{15}$ measured at 550 °C in air.

function of the atmosphere (oxygen, air or nitrogen). The conductivity increases with a decrease in oxygen pressure (from O_2 to N_2), whereas the corresponding activation energies (Table 1) changed in the reverse sequence. This result indicates the existence of electron conductivity. The electronic component can arise either from trapped or freshly generated oxygen vacancies. In the present investigation, the presence of the former is impossible since the sample was equilibrated at 400 °C for an extended period. Adopting the premise of George and Virkar in their study of the transport properties of $LaNb_3O_9$,[20] the structure of $Ba_5Nb_4O_{15}$ can be regarded as built up of corner-shared Nb–O octahedra oriented perpendicular to the *c*

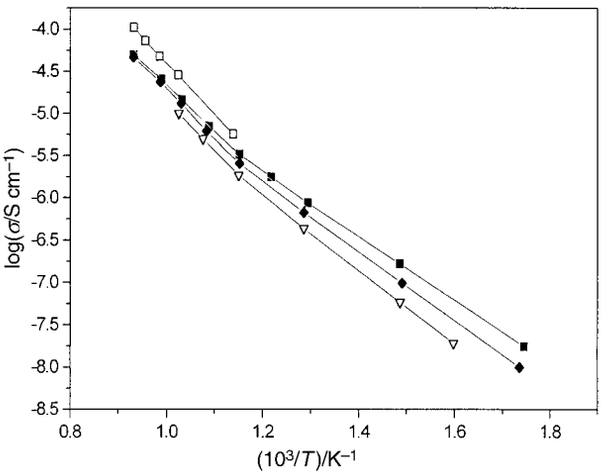

Fig. 7 ac Conductivity as a function of temperature for different atmospheres: (■) nitrogen, (◆) air, (▽) oxygen, (□) wet nitrogen.

Table 1 Conductivities and activation energies calculated at different measurement atmospheres and temperatures

Measurement atmosphere	Conductivity/S cm^{-1}		Activation energy/eV	
	600 °C	800 °C	<600 °C	>600 °C
Nitrogen	3.93×10^{-6}	5.49×10^{-5}	0.33	0.51
Air	2.69×10^{-6}	4.57×10^{-5}	0.36	0.49
Oxygen	2.08×10^{-6}	1.25×10^{-5}[a]	0.39	0.55
Wet nitrogen	5.89×10^{-6}	1.10×10^{-4}	—	0.62

[a]Measured at 700 °C.

axis and separated by BaO_{12} polyhedra,[4] and electron generation can be considered in terms of the structural instability of Nb–O octahedra in $Ba_5Nb_4O_{15}$.

Oxygen loss at 600 °C may influence the conductivity properties of $Ba_5Nb_4O_{15}$. To understand the mechanism, we investigated the isothermal conductivity of the oxide as a function of oxygen partial pressure at 800 °C. The conductivity decreases with an increase in oxygen pressure (Fig. 8) and analysis of the data yields eqn. (1):

$$\sigma = k{P_{O_2}}^{-1/6} \quad (1)$$

This dependence of conductivity on the partial pressure of oxygen indicates an *n*-type conduction behaviour at high temperatures, due to the formation of ionized oxygen vacancies

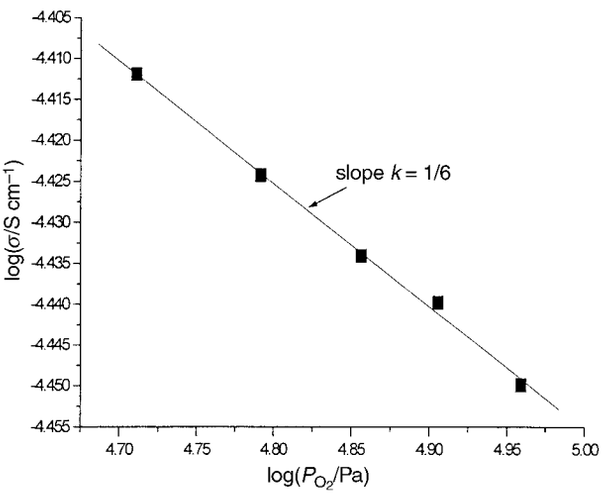

Fig. 8 Isothermal conductivity of $Ba_5Nb_4O_{15}$ plotted as a function of oxygen partial pressure.

in the lattice.[21] Loss of oxygen would cause the formation of oxygen vacancies in the lattice. The whole process involved can be expressed by eqns. (2)–(4)

$$O_O^X = V_O^X + 0.5O_2(g) \quad (2)$$

$$V_O^X = V_O^{\cdot} + e' \quad (3)$$

$$V_O^{\cdot} = V_O^{\cdot\cdot} + e' \quad (4)$$

Where O_O^X, V_O^X, $V_O^{\cdot}$ and $V_O^{\cdot\cdot}$ represent an oxygen ion on a normal lattice site, a neutral oxygen ion (anion) vacancy, a singly ionized anion vacancy and a doubly ionized anion vacancy, respectively. Assuming that complete ionization of oxygen vacancies occurs at high temperatures and the mass law is applied where reaction (4) is dominant, the reaction between the conductivity and partial pressure of oxygen can be given by eqn. [1].[22] Therefore, it is confirmed that doubly ionized oxygen vacancies are the predominant defects at high temperatures and electron conductivity arises from the movement of generated electrons.

When the sample is exposed to wet nitrogen, however, the conductivity increases dramatically and increases linearly with increase in partial water vapor pressure (Fig. 9), as observed in many other proton conductors.[23] Elimination of oxygen vacancies by water may occur according to eqn. (5):

$$H_2O_{(g)} + V_O^{\cdot\cdot} + O_O^X = 2OH_O^{\cdot} \quad (5)$$

This leads to a dramatic increase in hydroxyl radical concentration and proton conduction predominates in wet nitrogen at high temperatures. The conductivity of $Ba_5Nb_4O_{15}$ at 800 °C is 1.1×10^{-4} S cm^{-1} in wet nitrogen, two magnitude lower than that of doped $BaCeO_3$.[24] Although hydroxyl radicals are generated in the lattice, the structure of $Ba_5Nb_4O_{15}$ remains unchanged in a wet atmosphere at high temperatures *ca.* (800 °C). This is in contrast to $BaCeO_3$, which is thermodynamically unstable in wet atmospheres and decomposes between 500 and 900 °C.[25]

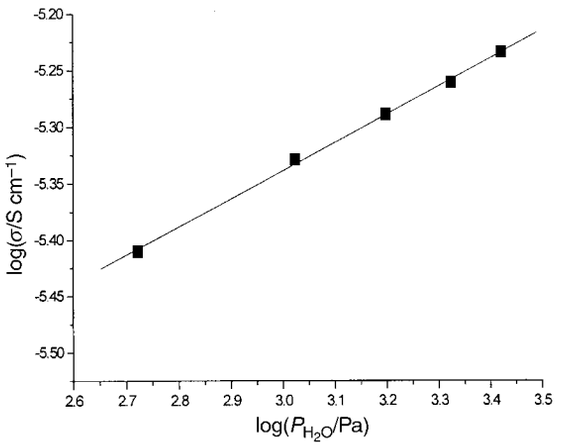

Fig. 9 ac Conductivity of $Ba_5Nb_4O_{15}$ as a function of water partial pressure (measured in a stream of nitrogen).

4 Conclusions

Pure phase $Ba_5Nb_4O_{15}$ is rapidly synthesized in 3 h by a hydrothermal method at 240 °C. The product is well crystallized and consists of ultrafine particles (*ca.* 100 nm). Mixed proton and electron conduction is observed for $Ba_5Nb_4O_{15}$. Structural instability and oxygen loss are the major factors for electron conduction in the temperature range 300–800 °C. In wet nitrogen, however, improved conduction arises from reaction of oxygen vacancies with water molecules. Compared with doped $BaCeO_3$, hydrothermally synthesized $Ba_5Nb_4O_{15}$ was more stable in a wet atmosphere at high temperatures, although its proton conductivity was relatively low (*ca.* 10^{-4} S cm^{-1}. The proton derives from reaction of water with oxygen vacancies, above 600 °C. Therefore, increasing the number oxygen vacancies in the lattice by suitable substitution of low valence elements may improve the proton conductivity.

References

1 F. L. Chen, O. T. Sorensen, G. Y. Meng and D. K. Peng, *J. Mater. Chem.*, 1997, **7**, 481.
2 K. C. Liang, Y. Du and A. S. Nowick, *Solid State Ionics*, 1994, **69**, 117.
3 F. Galasso and L. Katz, *Acta Crystallogr.*, 1961, **14**, 647.
4 A. M. Srivastava, J. F. Ackerman and W. W. Beers, *J. Solid State Chem.*, 1997, **134**, 187.
5 C. Vineis, P. K. Davies, T. Negas and S. Bell, *Mater. Res. Bull.*, 1996, **31**, 431.
6 H. Sreemoolanadhan, M. T. Sebastian and P. Mohanan, *Mater. Res. Bull.*, 1995, **30**, 653.
7 J. L. Hutchinson and A. J. Jacobson, *Acta Crystallogr., Sect. B*, 1975, **31**, 1442.
8 H. Sreemoolanadhan, Isaac. J. Solomon, S. M. T. Sebastian, K. A. Jose and P. Mohanan, *Phys. Status Solidi A*, 1994, **143**, K45.
9 N. E. Massa, S. Pagola and R. Carbonio, *Phys. Rev. B: Condens. Matter*, 1996, **53**, 8148.
10 P. P. Phule and S. H. Risbud, *J. Mater. Sci.*, 1990, **25**, 1169.
11 S. Feng and M. Greenblatt, *Chem. Mater.*, 1992, **4**, 462.
12 S. Feng, M. Tsai, S. Shi and M. Greenblatt, *Chem. Mater.*, 1992, **4**, 468.
13 S. Feng and M. Greenblatt, *Chem. Mater.*, 1993, **5**, 1277.
14 C. Zhao, S. Feng, Z. Chao, C.-S. Shi, R. Xu and Z. Ni, *Chem. Commun.*, 1996, 1941.
15 H. Zhao and S. Feng, *Chem. Mater.*, 1999, **11**, 958.
16 P. K. Dutta, R. Asiaie, S. A. Akbar and W. Zhu, *Chem. Mater.*, 1994, **6**, 1542.
17 R. S. Roth and J. L. Waring, *J. Res. Natl. Bur. Stand., Sect. A*, 1961, **65**, 337.
18 G. Blasse and A. F. Corsnit, *J. Solid State Chem.*, 1973, **6**, 513.
19 R. A. Nyquist and R. O. Kagel, in *Infrared Spectra of Inorganic Compounds*, Academic Press, New York, 1971.
20 A. M. George and A. N. Virkar, *J. Phys. Chem. Solids*, 1988, **49**, 743.
21 C. J. Kevane, *Phys. Rev. A*, 1964, **133**, 1431.
22 E. H. Greener, D. H. Whitmore and M. E. Fine, *J. Chem. Phys.*, 1961, **34**, 1017.
23 M. Sato, T. Jin and K. Uematsu, *J. Solid State Chem.*, 1993, **102**, 557.
24 H. Iwaharo, H. Uchida, K. Ono and K. Ogaki, *J. Electrochem. Soc.*, 1988, **135**, 529.
25 C. W. Tanner and A. V. Virkar, *J. Electrochem. Soc.*, 1996, **143**, 1386.

Paper a909554c